Supporting Information: Revisiting the mechanism of long-lived luminescence in host/guest organic crystals

Raphael B. Rullan,[†] Catherine Demangeat,[‡] Anthony D'Aléo,[¶,§] André-Jean Attias,[‖] Stephan N. Steinmann,[*,†] and Tangui Le Bahers[*,†,⊥]

†*ENS de Lyon, CNRS, LCH, UMR 5182, 69342, Lyon cedex 07, France*

‡*Department of Engineering Science, The University of Electro-Communications, 1-5-1 Chofugaoka, Chofushi, 1828585, Tokyo, Japan.*

¶*Institut de Physique et Chimie des Matériaux de Strasbourg (IPCMS), UMR 7504, CNRS-Université de Strasbourg, 23 Rue du Loess, 67034 Strasbourg Cedex 2, France*

§*Department of Physics, Ewha Womans University, Seoul 03760, Republic of Korea*

‖*Sorbonne Université, CNRS, MONARIS – UMR 8233, Paris, F-75005 France*

⊥*Institut Universitaire de France, Paris, France*

E-mail: stephan.steinmann@ens-lyon.fr; tangui.le_bahers@ens-lyon.fr

Contents

S1 Experimental section

S1.1 Reagents and materials

Unless otherwise stated, all reagents used in the experiments were purchased from commercial sources without further purification.

S1.2 Experimental methods

Nuclear magnetic resonance (^{1}H and ^{13}C) spectra were obtained on a Bruker Ultra Shield 300 MHz spectrometer for $CDCl_3$. Chemical shift was relative to tetramethylsilane as the internal standard. Resonance patterns are reported with the notation s (singlet), d (double), t (triplet), and m (multiplet).

LC-MS analysis: Chromatographic analysis was performed by an LC-MS system (Agilent, USA), an Agilent 1290 Infinity Binary LC with UV–vis photodiode array detector (DAD G4212A), coupled with an Agilent 6530 Accurate-Mass Quadrupole Time-of-Flight with a dual spray ESI source. G1316C Thermostatted column was set at 45 °C and two channel of elution solvents were water (A) and methanol (B), with 0.1% in volume of formic acid, respectively. Flow rate was 0.350 mL/min, injection volume was 20.00 μL (100 ppm), and column pressure was 600 bar as source parameters. The eluent conditions were (1) from 0 to 2 min with 10% B for isocratic condition, (2) from 10% to 100% B for 8 min for gradient condition, (3) 100% B for 3 min for isocratic condition, (4) from 100% to 90% B for 0.5 min for gradient condition, and (5) 90% B for 1.5 min for isocratic condition. Electrospray ionization mass spectrometric analysis (scan parameters) was performed in positive mode with nebulizer at temperature of 350 °C, flow of 10 L/min, pressure of 45 psi, capillary voltage of 3500 V, fragmentor voltage of 135 V, skimmer voltage of 65 V, octopole RF peak of 750 V, and sheath gas temperature (295 °C) and flow (11 L/min). A reference solution of the reference mass m/z 922.00979800 was used for continuous calibration. All data acquisition and analysis were managed by Agilent Mass Hunter Workstation Software (Agilent, USA).

The PLQY values of the crystalline powders were measured using an integrating sphere system coupled with a photonic multichannel analyzer (Hamamatsu Photonics C9920-02, PMA-11). The phosphorescence lifetimes were recorded with a SPEX Fluorolog 3 spectrometer.

S2 Synthesis

Cz-based matrices were prepared either from pure carbazole (prepared in a two steps sequence according to the procedure of Tian et al.[S1]) or (commercial) 2,7-dimethoxycarbazole through a two steps procedure combining (i) the preparation of the acetylenic carbazole precursor and (ii) its subsequent cross-coupling with the desired bromo-iodopyridine according to the following scheme. Some of these procedures have been described in earlier reports.[S2]

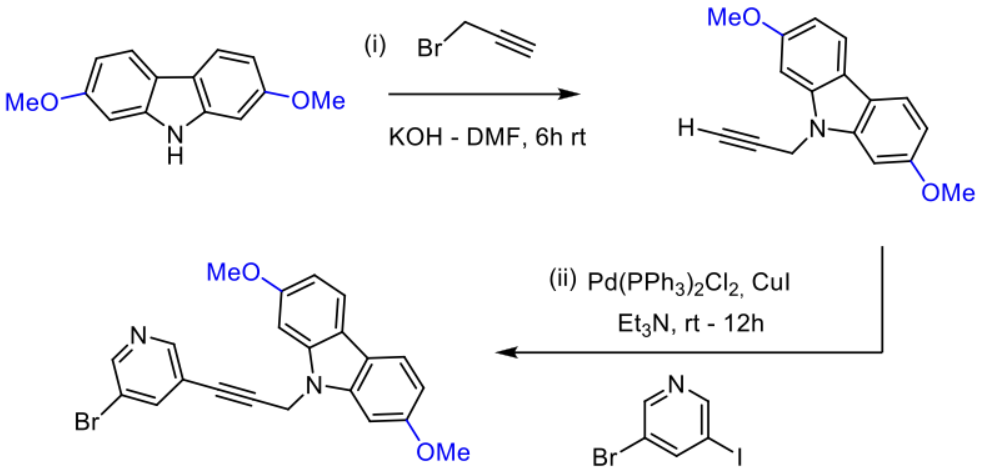

Figure S1: Two-steps synthetic route for the preparation of CzT24-OMe

S2.1 Synthesis of 2,7-dimethoxy-9-(prop-2-yn-1-yl)-9H-carbazole

To a solution of 2,7-dimethoxycarbazole (0.34 g, 1.5 mmol) in DMF (10 mL) was added solid KOH (0.17 g, 3.0 mmol, 2 equiv) at 0 °C. After 20 min. stirring at this temperature, propargyl bromide (80 % solution in toluene – 0.33 mL, 3.0 mmol, 2 equiv) was added. The reaction

was allowed to stir for a further 6 h at room temperature before water (20 mL) was added. The mixture was extracted with AcOEt (3 x 10 mL) and the combined organic layer dried over $CaCl_2$. The solvent were removed under reduced pressure and the crude product chromatographed using EtOAc/n-hexane - 1/9 as eluent, yielding the desired product which was further purified upon recrystallization to give 2,7-dimethoxy-9-(prop-2-yn-1-yl)-9H-carbazole (246 mg, 62 %) as white crystals.

S2.2 Sonogashira cross coupling of 2,7-dimethoxy-9-(prop-2-yn-1-yl)-9H-carbazole with corresponding bromo-iodopyridines (synthesis of CzT24-OMe)

Into a flame dried 100 mL two-necked flask were added $Pd(PPh_3)_2Cl_2$ (0.06 g, 0.085 mmol) CuI (0.03 g, 0.17 mmol), 3-bromo-5-iodopyridine (0.48 g, 1.7 mmol), 2,7-dimethoxy-9-(prop-2-yn-1-yl)-9H-carbazole (0.45 g, 1.7 mmol) and triethylamine (8 mL) under a nitrogen atmosphere. After stirring at room temperature for 12 h, water (10 mL) was added and the mixture was extracted with AcOEt (3 x 10 mL). The combined organic layers were dried over $CaCl_2$, and the solvents were removed under reduced pressure. The crude product was purified under column chromatography using $CHCl_3$/n-hexane – 8/2 as eluent to afford the expected product as colorless needlelike crystals (0.61 g 85%).

^{1}H NMR (300 MHz, $CDCl_3$): 8.56 (d, J = 2.2 Hz,1H); 8.50 (d, J = 1.6 Hz, 1H); 7.88 (s, 1H) ; 7.85 (s, 1H); 7.78 (t, J = 2.0 Hz, ^{1}H); 6.95 (d, J = 2.1 Hz, 2H); 6.88 (d, J = 2.2 Hz, 1H); 6.85 (d, J = 2.2 Hz, 1H); 5.17 (s, 2H); 3.94 (s, 6H).^{13}C NMR (300 MHz, $CDCl_3$): 158.41; 150.40; 141.27; 141.04; 120.85; 117.38; 93.72; 88.06; 79.32; 55.81; 33.03. LC-MS analysis: Calcd for $C_{22}H_{17}BrN_2O_2$: 420.0473. Found [M+H]+ : 421.05380

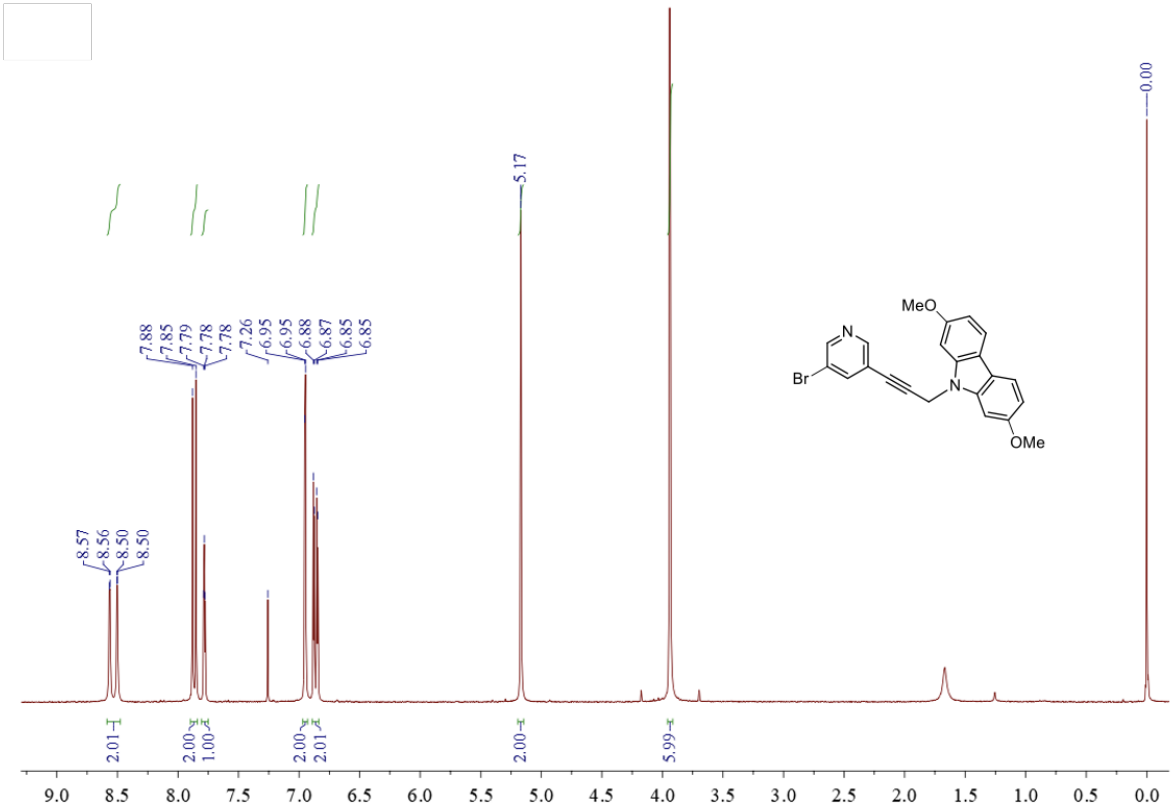

Figure S2: ^{1}H NMR spectrum of CzT24-OMe in $CDCl_3$

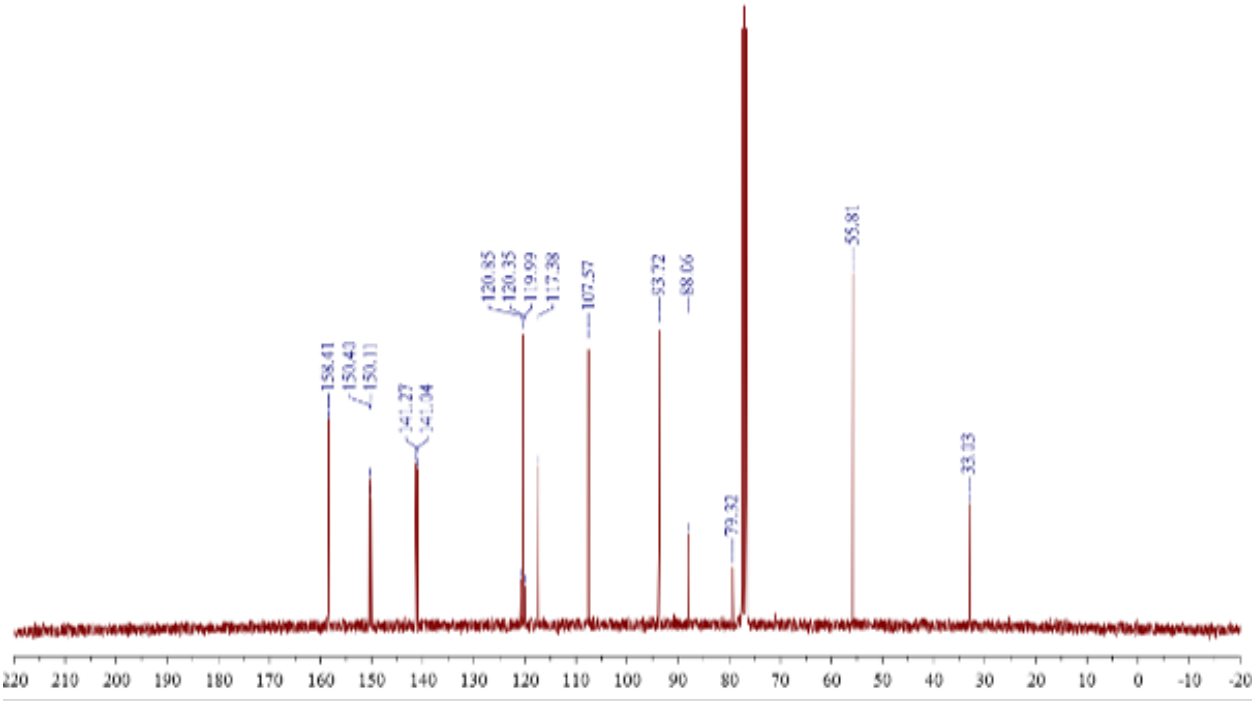

Figure S3: ^{13}C NMR spectrum of CzT24-OMe in $CDCl_3$

S3 Single crystals X-Ray diffraction analysis

Table S1: Crystal data and structure refinement for CzT24-OMe. CCDC deposit number: 2523899.

Identification code	CzT24-OMe	
Empirical formula	$C_{22}H_{17}BrN_2O_2$	
Formula weight	421.28	
Temperature	223(2) K	
Wavelength	0.71073 Å	
Crystal system	Monoclinic	
Space group	C2/c	
Unit cell dimensions	a = 29.95(2) Å	$\alpha = 90°$
	b = 4.094(3) Å	$\beta = 110.37(2)°$
	c = 31.31(2) Å	$\gamma = 90°$
Volume	3600(4) $Å^3$	
Z	8	
Density (calculated)	1.555 mg/m^3	
Absorption coefficient	2.304 mm^{-1}	
F(000)	1702	
Crystal size	0.185 × 0.071 × 0.050 mm^3	
θ range for data collection	2.331 to 28.425°	
Index ranges	-39 ≤ h ≤ 40, -5 ≤ k ≤ 5, -41 ≤ l ≤ 41	
Reflections collected	19462	
Independent reflections	4530 [R(int) = 0.0889]	
Completeness to $\theta = 25.242°$	99.9%	
Absorption correction	Semi-empirical from equivalents	
Max. and min. transmission	0.7457 and 0.6584	
Refinement method	Full-matrix least-squares on F^2	
Data / restraints / parameters	4530/0/245	
Goodness-of-fit on F2	0.993	
Final R indices [I>2σ(I)]	R1 = 0.0498, ωR2 = 0.0896	
R indices (all data)	R1 = 0.1321, ωR2 = 0.1178	
Extinction coefficient	n/a	
Largest diff. peak and hole	0.315 and -0.320 e. $Å^{-3}$	

S4 Study of the ground state properties: understanding the electronic structure

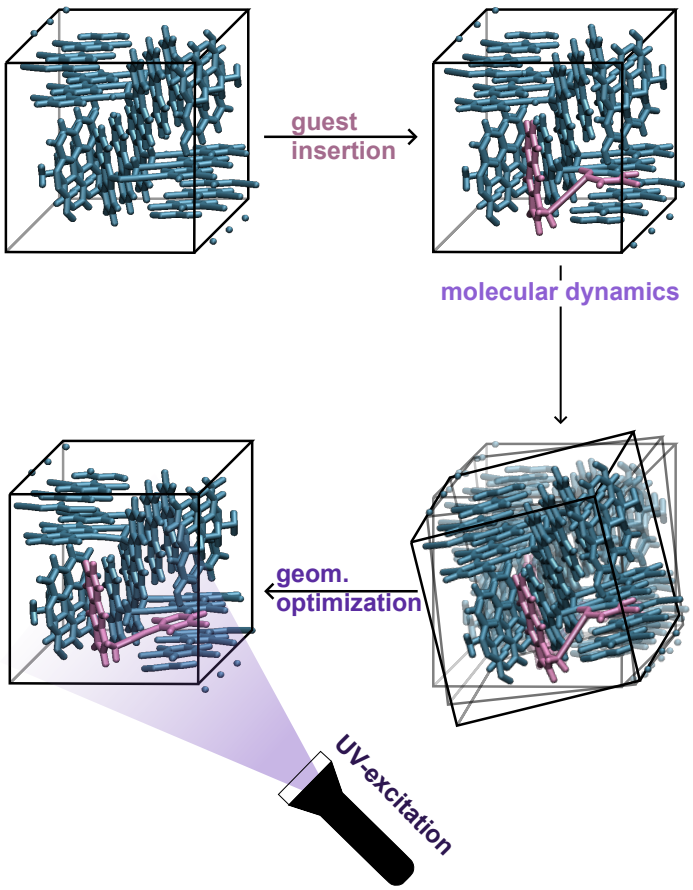

Figure S4: Scheme of the geometry optimization

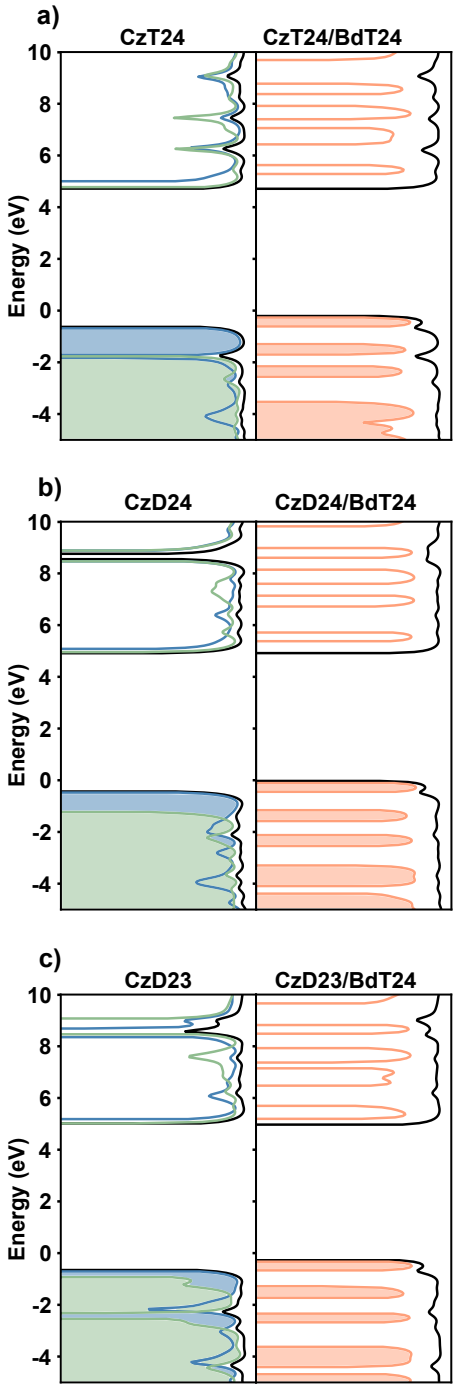

Figure S5: Computed DOS for the pure Cz-based hosts and the BdT24-doped hosts using the CAM-B3LYP functional. Projection on the Cz, the pyridine and the Bd are in blue, green and orange respectively. The filled bands correspond to occupied states and the empty ones to empty states. The DOS are presented in the log scale. The black line corresponds to the total DOS.

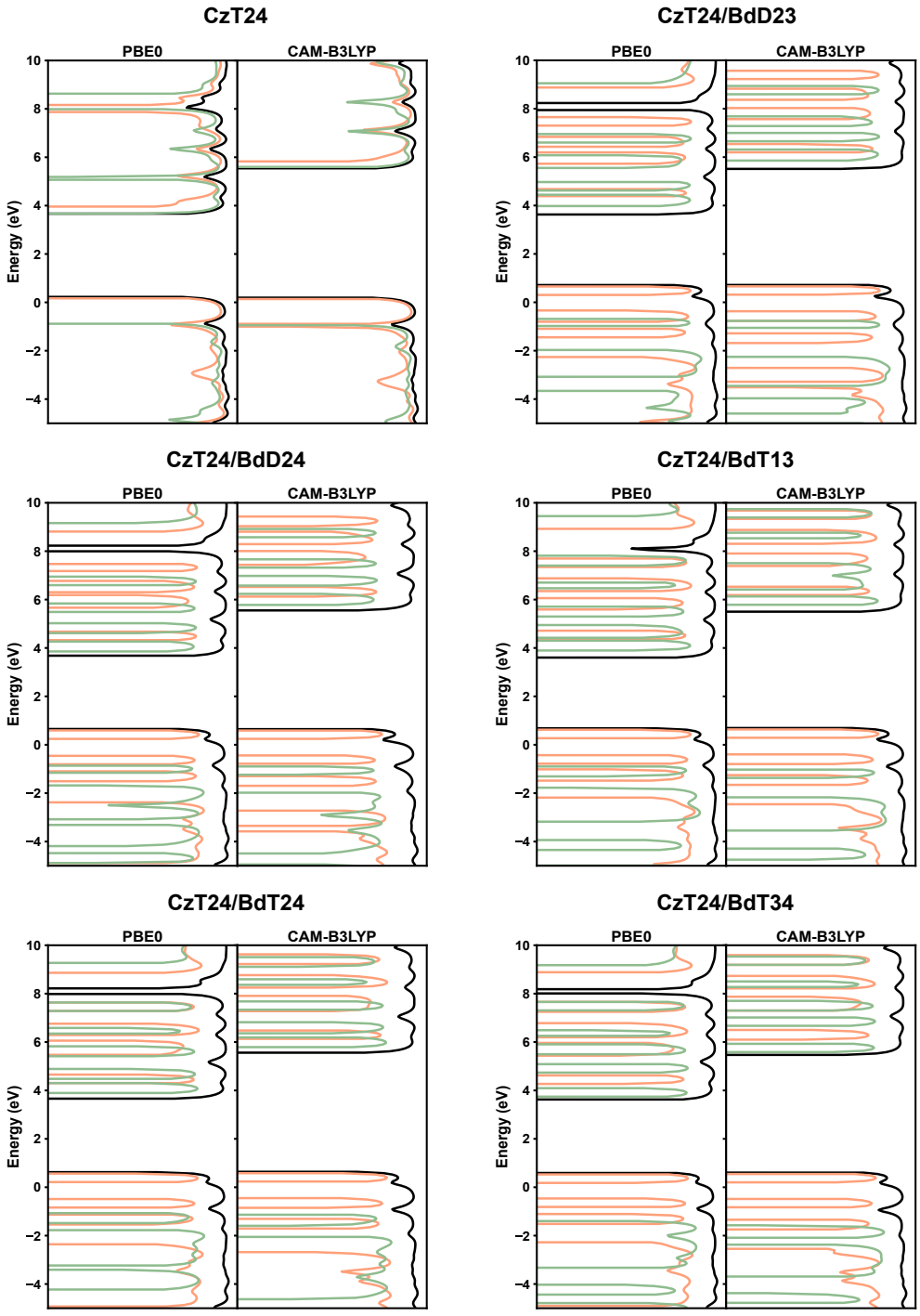

Figure S6: Comparison between DOS for all systems with the CzT24 matrix using the PBE0 and CAM-B3LYP functionals. Projection on the pyridine of the defect and the Bd are in green and orange respectively. For the pure system, the orange bands corresponds to the projection on the carbazoles and the green bands onto the pyridines. The DOS are presented in the log scale. The black line corresponds to the total DOS.

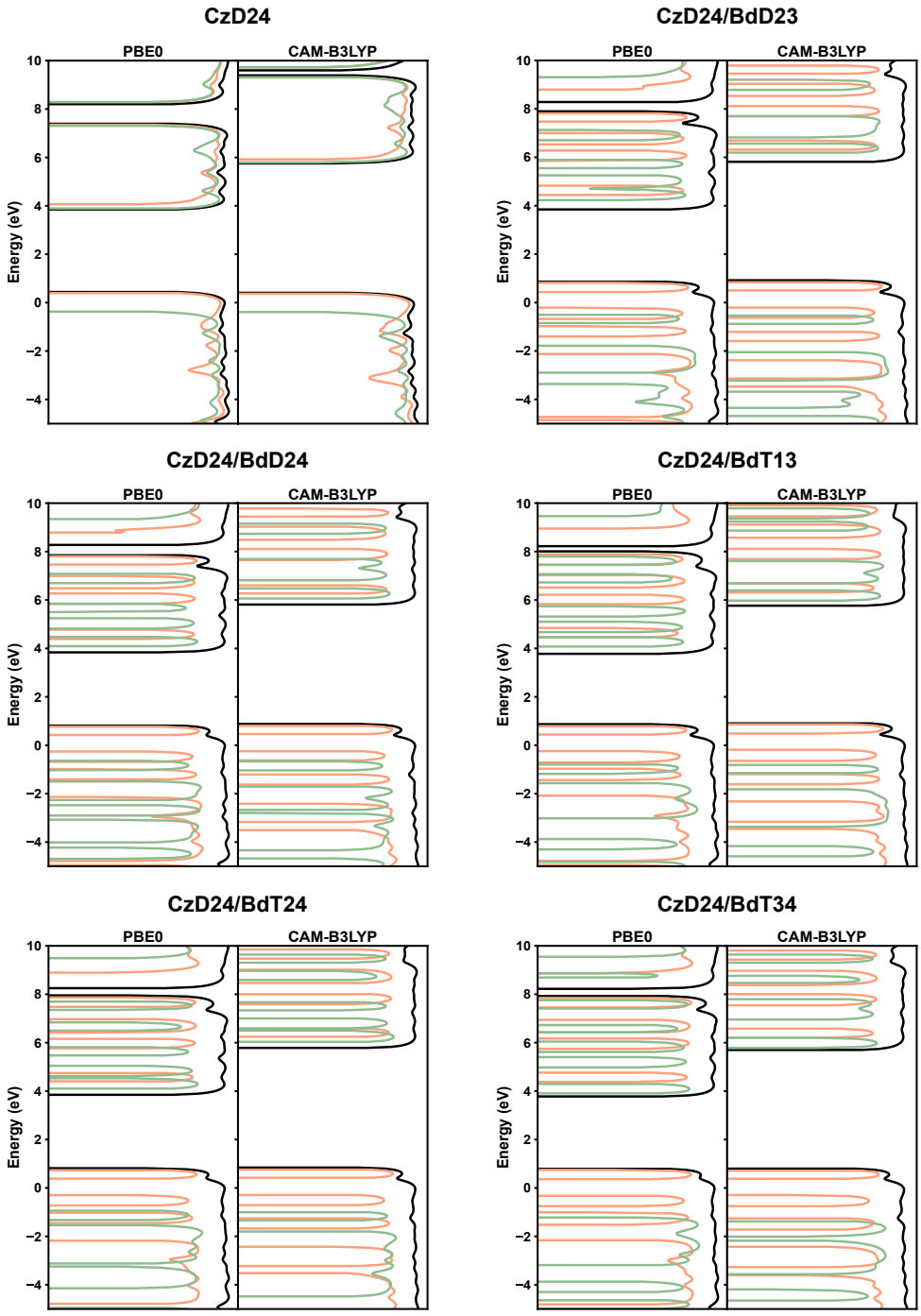

Figure S7: Comparison between DOS for all systems with the CzD24 matrix using the PBE0 and CAM-B3LYP functionals. Projection on the pyridine of the defect and the Bd are in green and orange respectively. For the pure system, the orange bands corresponds to the projection on the carbazoles and the green bands onto the pyridines. The DOS are presented in the log scale. The black line corresponds to the total DOS.

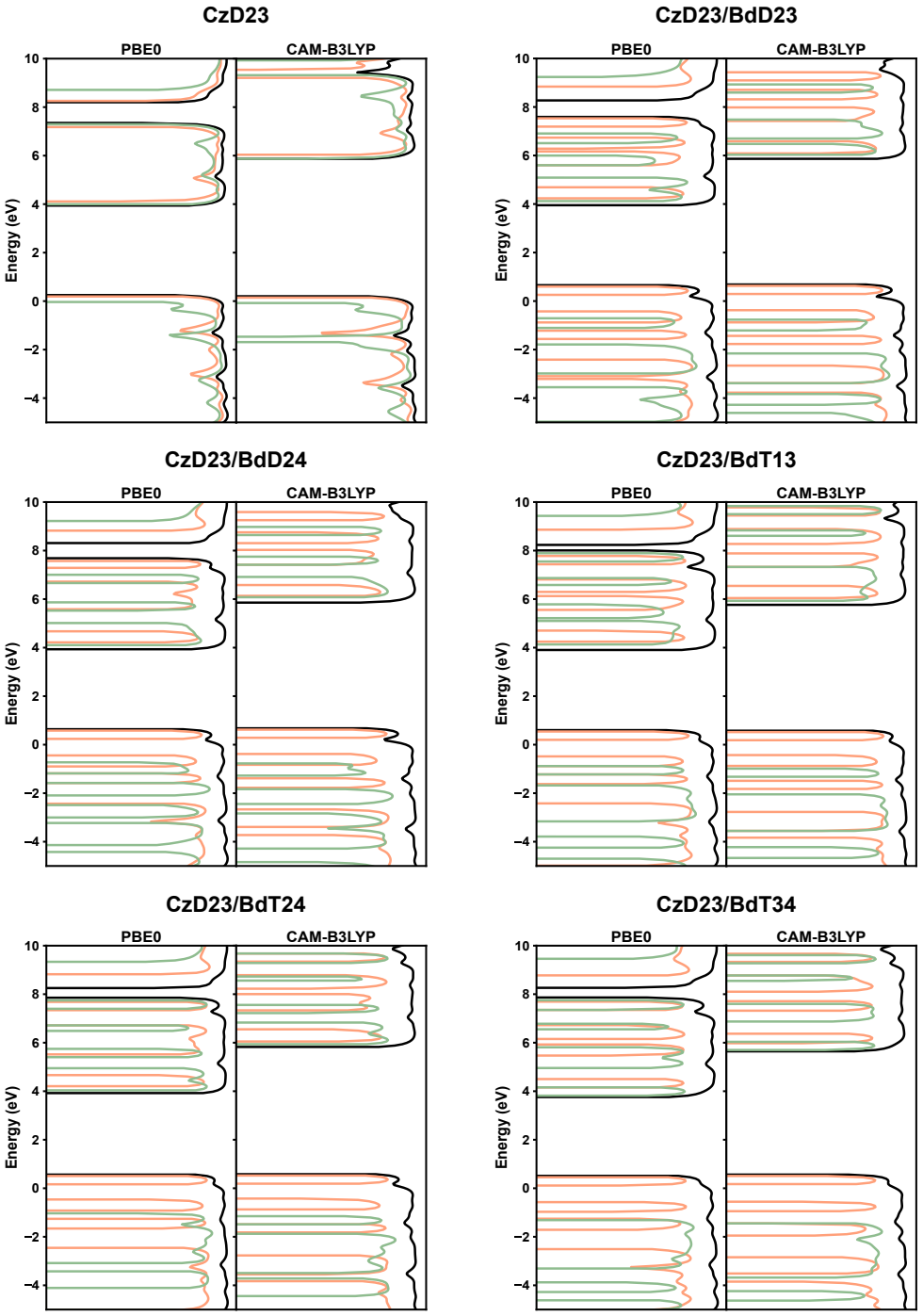

Figure S8: Comparison between DOS for all systems with the CzD23 matrix using the PBE0 and CAM-B3LYP functionals. Projection on the pyridine of the defect and the Bd are in green and orange respectively. For the pure system, the orange bands corresponds to the projection on the carbazoles and the green bands onto the pyridines. The DOS are presented in the log scale. The black line corresponds to the total DOS.

S5 ALMO for investigating targeted triplet states

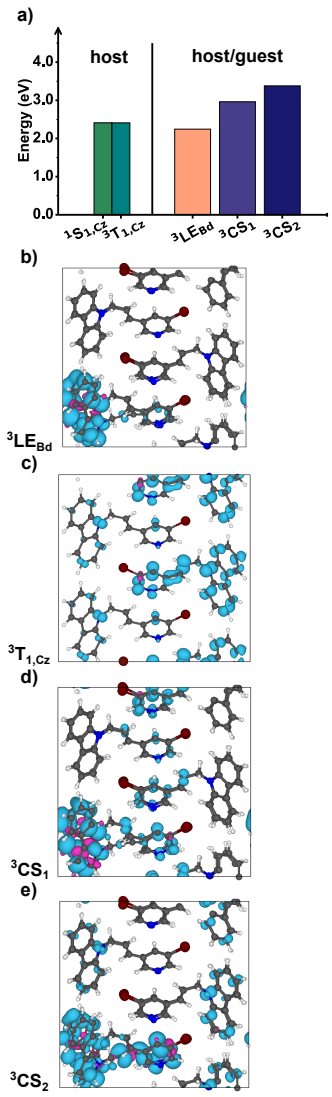

Figure S9: a) Representation of the energies of the singlet $^1S_{1,Cz}$ and of the triplet $^3T_{1,Cz}$ of the host CzD24 computed using TD-DFT. ΔSCF energies of different triplet states $^3LE_{Bd}$, $^3CS_1$ and $^3CS_2$ of the host-guest system CzD24/BdT24 computed using ALMO. b) Spin density of the $^3LE_{Bd}$ state. c) Spin density of the non-ALMO computation for the CzD24 host. d) Spin density of the $^3CS_1$ state. e) Spin density of the $^3CS_2$ state.

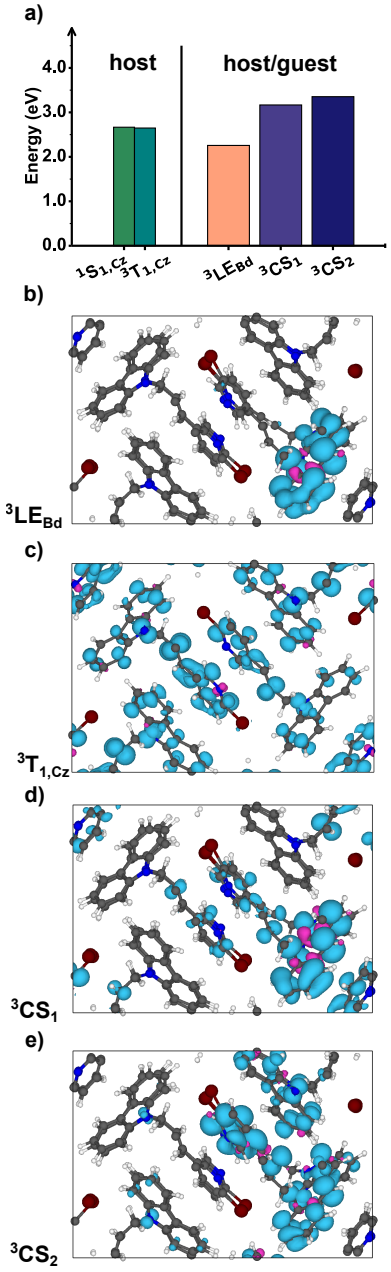

Figure S10: a) Representation of the energies of the singlet $^1S_{1,Cz}$ and of the triplet $^3T_{1,Cz}$ of the host CzD23 computed using TD-DFT. ΔSCF energies of different triplet states $^3LE_{Bd}$, $^3CS_1$ and $^3CS_2$ of the host-guest system CzD23/BdT24 computed using ALMO. b) Spin density of the $^3LE_{Bd}$ state. c) Spin density of the non-ALMO computation for the CzD23 host. d) Spin density of the $^3CS_1$ state. e) Spin density of the $^3CS_2$ state.

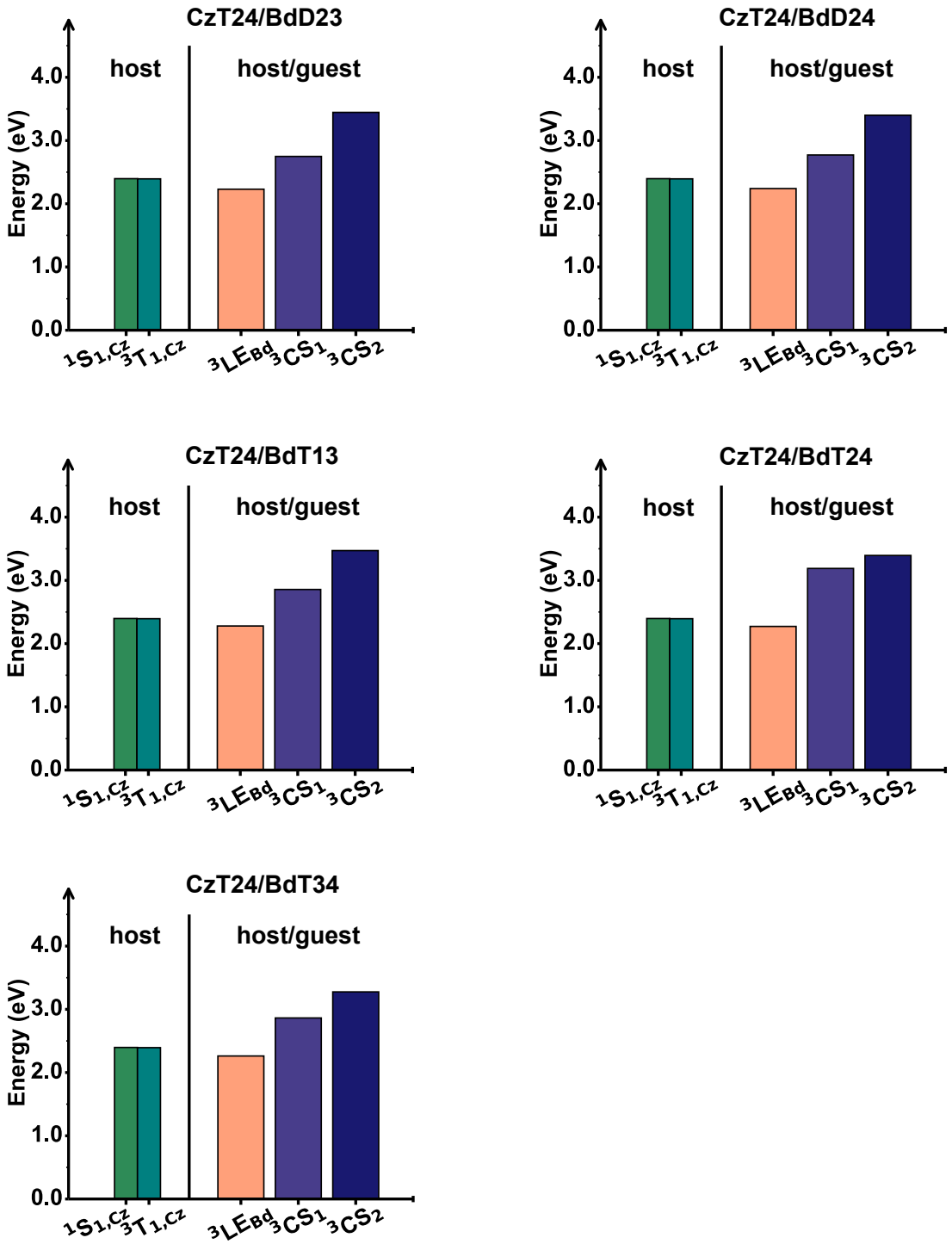

Figure S11: Representation of the energies of the singlet $^1S_{1,Cz}$ and of the triplet $^3T_{1,Cz}$ of the host CzT24 computed using TD-DFT. ΔSCF energies of different triplet states $^3LE_{Bd}$, $^3CS_1$ and $^3CS_2$ for all the host-guest system with the CzT24 host computed using ALMO.

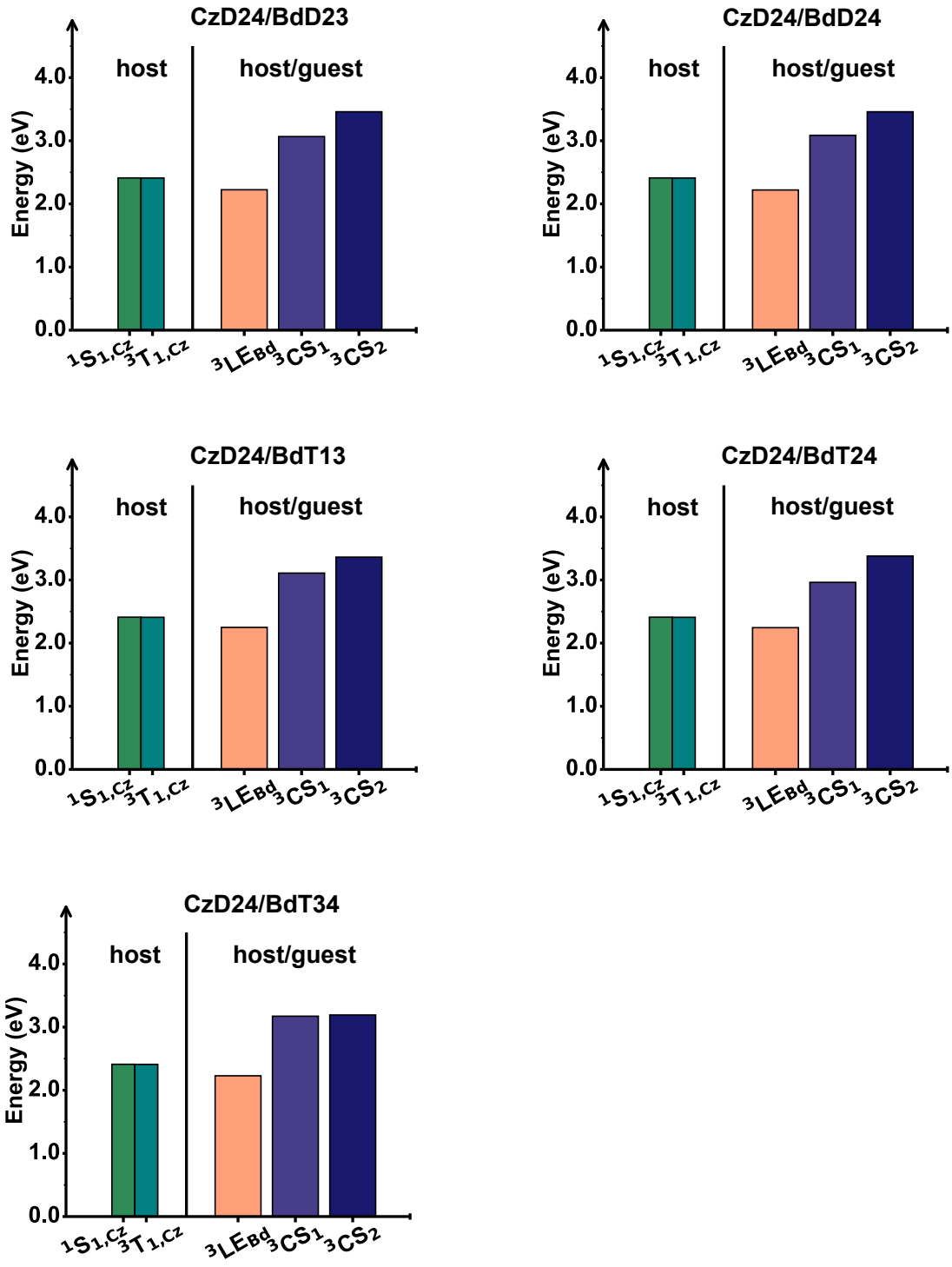

Figure S12: Representation of the energies of the singlet $^1S_{1,Cz}$ and of the triplet $^3T_{1,Cz}$ of the host CzD24 computed using TD-DFT. ΔSCF energies of different triplet states $^3LE_{Bd}$, $^3CS_1$ and $^3CS_2$ for all the host-guest system with the CzD24 host computed using ALMO.

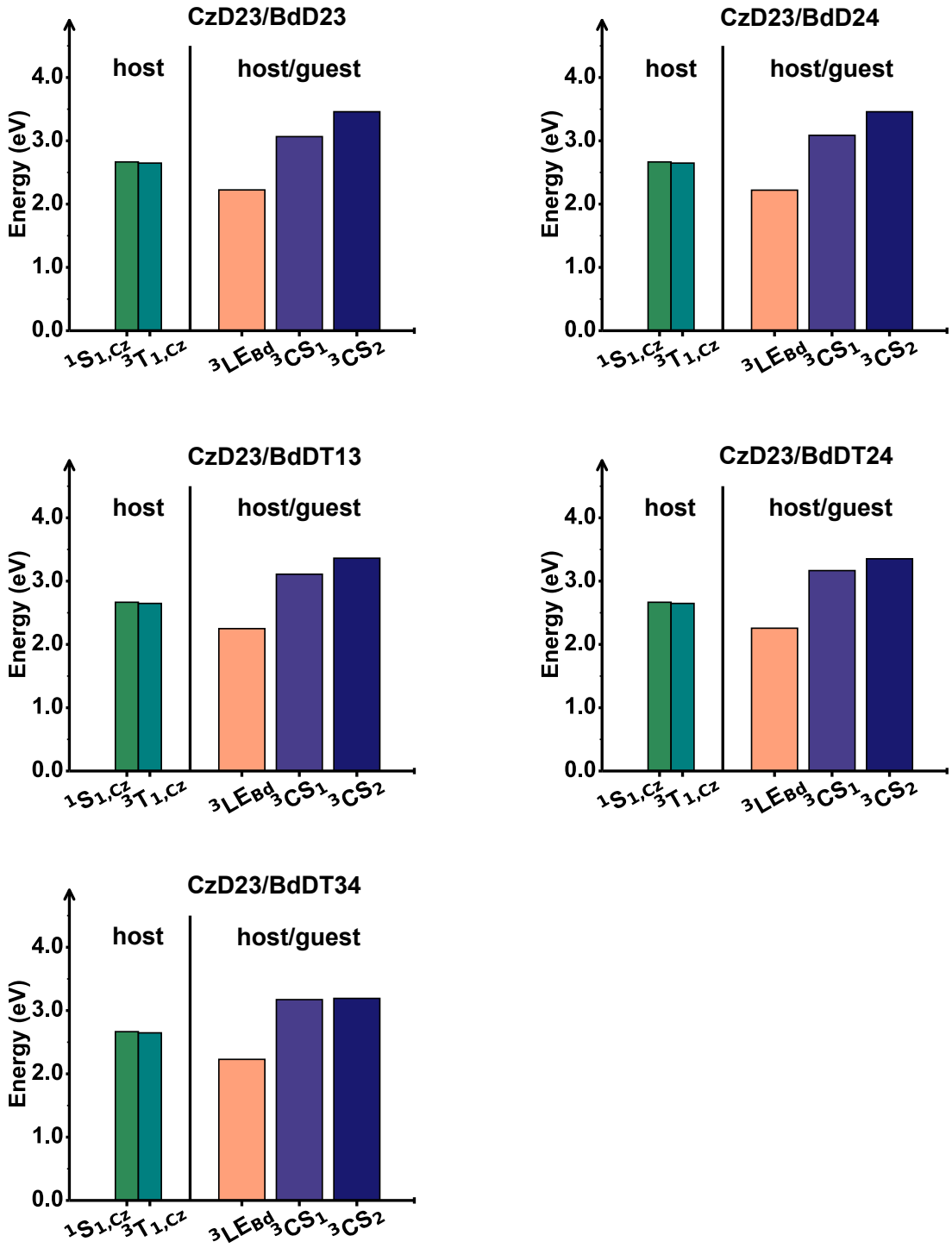

Figure S13: Representation of the energies of the singlet $^1S_{1,Cz}$ and of the triplet $^3T_{1,Cz}$ of the host CzD23 computed using TD-DFT. ΔSCF energies of different triplet states $^3LE_{Bd}$, $^3CS_1$ and $^3CS_2$ for all the host-guest system with the CzD23 host computed using ALMO.

S6 Investigation of SOC

The Orca program was used to compute the spin-orbit coupling (SOC) between all triplet states below the S_1 state at geometries extracted from the crystal strucure using the quadric-response TD-DFT in the Tamm-Dancoff approximation at the CAM-B3LYP/PCM level with the Def2-SVP-DK basis set adapted for the Douglas–Kroll hamiltonian.[S3–S5]

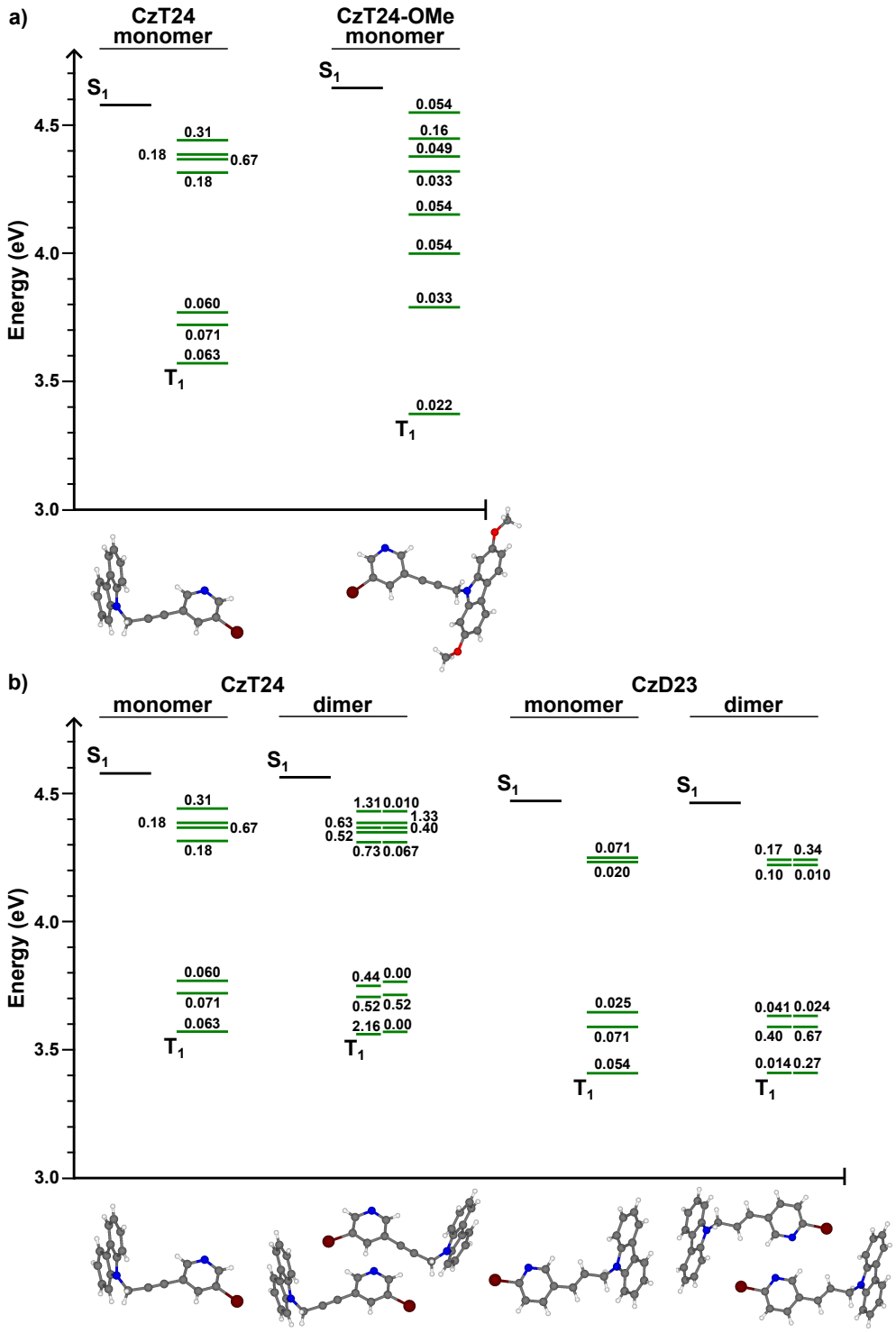

Figure S14: (a) TD-DFT computed excited state energies and S1-Tn SOC intensities (given in cm-1) of CzT24 and CzT24-OMe monomers extracted from the crystal structure. (b) TD-DFT computed excited state energies and S1-Tn SOC intensities (given in cm-1) of CzT24 and CzD23e monomers and dimers extracted from the crystal structure

References

(S1) Tian, X.; Song, L.; Hashmi, A. S. K. Synthesis of Carbazoles and Related Heterocycles from Sulfilimines by Intramolecular C-H Aminations. *Angew. Chem., Int. Ed.* **2020**, *59*, 12342–12346.

(S2) Demangeat, C.; Tang, Y.; Dou, Y.; Dale, S.; Cielo, J.; Kim, E.; Lee, H.-J.; D'Aléo, A.; Hu, B.; Attias, A.-J. Necessary and Sufficient Condition for Organic Room-Temperature Phosphorescence from Host–Guest Doped Crystalline Systems. *Adv. Opt. Mater.* **2023**, *11*, 2300289.

(S3) Neese, F.; Wennmohs, F.; Becker, U.; Riplinger, C. The ORCA quantum chemistry program package. *J. Chem. Phys.* **2020**, *152*, 224108.

(S4) Neese, F. Software update: The ORCA program system—Version 5.0. *Wiley Interdiscip. Rev. Comput. Mol. Sci.* **2022**, *12*, e1606.

(S5) Yanai, T.; Tew, D. P.; Handy, N. C. A new hybrid exchange–correlation functional using the Coulomb-attenuating method (CAM-B3LYP). *Chem. Phys. Lett.* **2004**, *393*, 51–57.